

RECEIVED: November 2, 2023

REVISED: March 11, 2024

ACCEPTED: March 30, 2024

PUBLISHED: April 19, 2024

A new method for calculating the soft anomalous dimension matrix for massive particle scattering

Johannes Henn^{},^a Calum Milloy^b and Kai Yan^{}^{c,d}

^a*Max-Planck-Institut für Physik, Werner-Heisenberg-Institut,
Boltzmannstr. 8, 80805 München, Germany*

^b*Dipartimento di Fisica and Arnold-Regge Center, Università di Torino
and INFN, Sezione di Torino,
Via P. Giuria 1, I-10125 Torino, Italy*

^c*INPAC, Shanghai Key Laboratory for Particle Physics and Cosmology,
School of Physics and Astronomy, Shanghai Jiao Tong University,
800 Dongchuan Road, Shanghai 200240, China*

^d*Key Laboratory for Particle Astrophysics and Cosmology (MOE),
800 Dongchuan Road, Shanghai 200240, China*

E-mail: henn@mpp.mpg.de, milloy@to.infn.it, yan.kai@sjtu.edu.cn

ABSTRACT: The general structure of infrared divergences in the scattering of massive particles is captured by the soft anomalous dimension matrix. The latter can be computed from a correlation function of multiple Wilson lines. The state-of-the-art two-loop result has a tantalizingly simple structure that is not manifest in the calculations. We argue that the complexity in intermediate steps of the known calculations comes from spurious, regulator-dependent terms. Based on this insight we propose a different infrared regulator that is associated to only one of the Wilson lines. We demonstrate that this streamlines obtaining the two-loop result: computing the required Feynman integrals via the differential equations method, only multiple polylogarithmic functions appear (to all orders in the dimensional regulator), as opposed to elliptic polylogarithms. We show that the new method is promising for higher-loop applications by computing a three-loop diagram of genuine complexity, and provide the answer in terms of multiple polylogarithms. The relatively simple symbol alphabet we obtain may be of interest for bootstrap approaches.

KEYWORDS: Factorization, Renormalization Group, Scattering Amplitudes, Wilson, 't Hooft and Polyakov loops

ARXIV EPRINT: [2310.10145](https://arxiv.org/abs/2310.10145)

Contents

1	Introduction	1
2	Definitions and discussion of the method	3
2.1	Soft anomalous dimension matrix	3
2.2	Proposal of a new infrared regularization procedure	5
3	The two-loop soft anomalous dimension matrix via the new method	8
3.1	One loop	8
3.2	Two loops	10
4	Three-loop calculation of a three-line web function	14
5	Discussion and outlook	18
A	Asymptotic expansion by regions for $\mathcal{S}_{\delta,\delta,1}$ at two-loop level	20

1 Introduction

Being able to predict the structure of infrared divergences in scattering processes is relevant for collider physics. For massless particles, the general structure of divergences is known to three loops. The infrared divergences factorize, similar to ultraviolet divergences. Due to color dependence, the infrared factorization takes the form of a matrix in color space. The essential part of the matrix is computed by the soft anomalous dimension matrix, which is determined from a correlation function of Wilson lines meeting at the origin, and pointing in the direction of the scattered particles' momenta [1–3].

Up to two loops the soft anomalous dimension matrix consists only of so-called dipole terms, which depend on pairs of scattered particles only [4–6]. Starting from three loops, correlations between multiple lines (in particular, four lines) are also present. Interestingly, the four-line correlations depend on a function of two scale-invariant ratios, which has been computed at three loops [7], and its presence has been confirmed in four-particle scattering amplitudes [8, 9].

The structure of infrared divergences of massive particles is more intricate. In the two-line case, the state of the art for the cusp anomalous dimension is three-loop order in QCD [10, 11] and four-loop order in QED [12]. Much less is known beyond the dipole terms. The two-loop soft anomalous dimension matrix involving three massive particles was computed by several groups [13–16]. The result includes a color structure beyond the dipole terms, namely $f^{abc}\mathbf{T}_i^a\mathbf{T}_j^b\mathbf{T}_k^c$, where \mathbf{T}_i^a is the colour matrix in the representation of particle i [17, 18]. (At higher loop orders, further color structures may appear.) The accompanying function depends on the scale invariant combination of the scalar products between the velocities of the particles,

$$\beta_{ij} = \frac{v_i \cdot v_j}{\sqrt{v_i^2} \sqrt{v_j^2}}. \tag{1.1}$$

The function multiplying this color structure depends on three variables of the type (1.1), since at two loops Feynman diagrams connect up to three Wilson lines, cf. figure 2. Remarkably, the result is much simpler than a genuine three-variable function: it takes the form of a sum over products of logarithms and dilogarithms that individually depend on one variable only.

This simplicity is not transparent in the state-of-the-art calculations. It is interesting to note that the calculations in the literature were done by different means, via Mellin-Barnes methods [14], by a position-space calculation [13, 15], and by a special gauge choice [16]. While all produce the correct result, it is not clear whether the methods can be easily generalized to the next loop order. Moreover, for the first two methods, the answer takes a simple form appears at the end of the calculation only. This motivates us to understand why this is the case, and to look for other approaches.

In recent years, the differential equation method [19–21] has proven extremely useful for the calculation of Feynman integrals, especially thanks to new ideas about the transcendental structure of Feynman integrals [22]. It is therefore interesting to see how the two-loop calculation would look like with this method. It turns out [23, 24] that the most complicated two-loop Feynman diagram, shown in figure 2(b), involves elliptic functions. This can be seen by a cut analysis, or by inspecting the differential equations matrix. What this means is that the $\mathcal{O}(1/\epsilon)$ part of the calculation, which contributes to the soft anomalous dimension matrix, is simple, but the higher order terms in the ϵ -expansion are much more complicated. Although extracting the relevant information from the complicated differential equations is possible [24], by carefully expanding them in ϵ , this is rather cumbersome. So, the question arises, is there a simpler approach?

It is important to realize that the soft anomalous dimension matrix corresponds to the leading divergence in ϵ of the Feynman integrals (or, linear combinations of Feynman diagrams organized in so-called webs [25–27]). In the calculations, a regularization choice is usually made to extract this divergence. In the language of position-space Wilson line correlators, the divergence we are interested in is a short-distance one, originating from webs of Feynman diagrams that homogeneously scale to zero towards the origin. This divergence is regulated by dimensional regularization, with $d = 4 - 2\epsilon$, and $\epsilon > 0$. The soft anomalous dimension matrix corresponds to the coefficient of the $1/\epsilon$ pole. However, the Wilson lines extend all the way to infinity, and this introduces a long-distance divergence that we are not interested in. It is common in the literature to regulate this by an exponential suppression factor. It is important to realize that due to the cutoff, only the leading $1/\epsilon$ pole is gauge-invariant and meaningful, while e.g. the finite term is not. So, it is no surprise that the functions contributing to the finite term can be very complicated — they do not have a physical meaning, and depend on the regularization procedure!

This motivates us to search for a different way of regulating the long-distance divergences of the webs. Our idea is the following: to make the webs well-defined, it is sufficient to regulate one of the Wilson lines with an exponential suppression factor. In this paper, we provide an argument why this procedure leads to the correct soft anomalous dimension matrix. We introduce the new method in section 2. We then show the effectiveness of the method in section 3, by easily reproducing the known two-loop result, and by computing the contribution of a previously unknown three-loop web function for the three-lines soft anomalous dimension matrix, in section 4. We discuss implications for prospects of future investigations in section 5.

2 Definitions and discussion of the method

2.1 Soft anomalous dimension matrix

Scattering amplitudes of massive particles contain infrared divergences due to virtual exchange of small quanta between heavy particles. In particular, an n -point gauge theory amplitude with massive external legs obeys a factorization formula which characterizes its all-loop infrared structure [1–6, 28–35],

$$\mathcal{M}_n(p_i, m_i, \mu; \alpha_s(\mu); \epsilon) = S_n(v_i; \alpha_s(\mu); \epsilon) H_n(p_i, m_i, \mu; \alpha_s(\mu)), \quad (2.1)$$

where S_n is the soft function encoding all the infrared singularities, and H_n collects the finite remainder of the amplitude \mathcal{M}_n . All quantities are renormalized with ultraviolet (UV) poles removed. The running coupling $\alpha_s(\mu)$ is evaluated at the scale μ in $\overline{\text{MS}}$ scheme. It satisfies the following equation in $d = 4 - 2\epsilon$ dimensions,

$$\frac{d \ln \alpha_s}{d \ln \mu} = -2\epsilon - 2 \sum_k \left(\frac{\alpha_s}{4\pi} \right)^k b_k. \quad (2.2)$$

The b_k coefficients are coefficients of the beta function $\beta(\alpha_s)$.

The S_n is a universal function depending on the velocities $v_i \equiv p_i/m_i$ of the scattering particles. It governs the singularity of the amplitudes both in the infrared region and in the infinite mass limit of the external particles, which can be studied in the context of Heavy Quark Effective Theory (HQET) (see, e.g. [36]). In the limit $m_Q \rightarrow \infty$, the heavy quark traveling with velocity v_i behaves like a classical source, whose interactions with soft gluons are represented by a Wilson line

$$Y_i(x) \equiv \mathbf{P} \exp \left[ig \int_0^\infty ds v_i \cdot A^a(x + v_i s) T^a \right]. \quad (2.3)$$

Hence S_n admits a formal definition as the correlation function of n semi-infinite Wilson lines emanating from the origin, whose renormalization group equation defines the corresponding soft anomalous dimension [1, 37–39],

$$S_n = \langle 0 | \prod_{i=1}^n Y_i(0) | 0 \rangle_{\text{ren.}}, \quad \frac{d}{d \ln \mu} S_n = -S_n \mathbf{\Gamma}_n. \quad (2.4)$$

The anomalous dimension $\mathbf{\Gamma}_n$ is a matrix operator in color space acting on the multi-point amplitudes. It can be expanded as a sum over dipole, tripole and quadrupole functions, etc, [14, 40–44]

$$\mathbf{\Gamma}_n(v_i; \alpha_s) = \sum_{(i,j)} \mathbf{\Gamma}_{ij}(x_{ij}; \alpha_s) + \sum_{(i,j,k)} \mathbf{\Gamma}_{ijk}(x_{ij}, x_{jk}, x_{ik}; \alpha_s) + \dots, \quad (2.5)$$

which are parametrized by the variables

$$v_i \cdot v_j \equiv \cosh \phi_{ij} \equiv -\frac{1}{2}(x_{ij} + 1/x_{ij}), \quad (2.6)$$

where we assume for simplicity $v_i^2 = 1$. The operators $\mathbf{\Gamma}_{ij\dots}$ come from multi-Wilson-line diagrams describing the interactions between Wilson lines labeled by i, j, \dots , and hence

depend on the associated color charges, as well as on the angles between the respective lines. The corresponding light-like soft anomalous dimension matrix (which is reached via $i\phi_{ij}'s \rightarrow \infty$) is known up to the three-loop order [7]. In this case, beyond-dipole terms vanish at two loops and begin at three loops. This is in contrary to the massive case, where beyond-dipole terms are already present at two loops.

The soft function obeys the exponentiation theorem for Wilson-line matrix elements, whose logarithm defines a web function free from sub-divergences in the infrared regime. More explicitly, it can be constructed through its α_s -expansion,

$$W(\alpha_s(\mu)) \equiv \log \langle Y_1 \cdots Y_n \rangle_{\text{ren.}} \tag{2.7}$$

$$= \log \left\{ 1 + \sum_{k=1}^{\infty} \left(\frac{\alpha_s(\mu)}{4\pi} \right)^k S_n^{(k)} \right\} \tag{2.8}$$

$$= \sum_{k=1}^{\infty} \left(\frac{\alpha_s(\mu)}{4\pi} \right)^k W^{(k)}. \tag{2.9}$$

In the abelian theory, e.g. QED, the L -loop web function determines the L -loop soft anomalous dimension through its evolution equation $\frac{d}{d \ln \mu} W_{\text{QED}}^{(L)} = -\Gamma_{\text{QED}}^{(L)}$. In particular, in the cases where all fermions are treated as massive, the abelian web function is one-loop exact. In the non-abelian theory like QCD, higher-loop web functions contain maximally non-abelian color structures, which, at a given loop order, vanish in the abelian theory and cannot be decomposed onto an abelian product of lower-loop color structures. More intuitively, the L -loop color factors can be associated with web diagrams containing $L - 1$ interaction vertices among the virtual soft particles. These non-abelian contributions give rise to multi-line color correlations in the web function.

We are interested in the tripole function Γ_{ijk} in the soft anomalous dimension. Up to the three-loop order it has the following structure, [14, 43]

$$\begin{aligned} \Gamma_{123} = & i f^{abc} \mathbf{T}_1^a \mathbf{T}_2^b \mathbf{T}_3^c F_1(x_{12}, x_{13}, x_{23}; \alpha_s) \\ & + \left\{ [\mathbf{T}_1^c, \mathbf{T}_1^a] [\mathbf{T}_2^b, \mathbf{T}_2^c] \{ \mathbf{T}_3^a, \mathbf{T}_3^b \} F_2(x_{12}, x_{13}, x_{23}; \alpha_s) + \right. \\ & \left. + (1, 2, 3) \rightarrow (2, 3, 1) + (1, 2, 3) \rightarrow (3, 1, 2) \right\}. \end{aligned} \tag{2.10}$$

Here the α_s -expansion of F_1 starts at the two-loop order, i.e.

$$F_1 = \sum_{k=2}^{\infty} \left(\frac{\alpha_s}{4\pi} \right)^k F_1^{(k)}, \tag{2.11}$$

and that of F_2 starts at three-loop order, i.e.

$$F_2 = \sum_{k=3}^{\infty} \left(\frac{\alpha_s}{4\pi} \right)^k F_2^{(k)}. \tag{2.12}$$

In the light-like limit, the all-order F_1 vanishes due to Bose symmetry, and $F_2^{(3)}$ reduces to a constant [7]. In this work we introduce a new method to compute the full angle-dependent functions $F_1^{(3)}$ and $F_2^{(3)}$.

2.2 Proposal of a new infrared regularization procedure

The factorization properties we just reviewed suggest that the soft anomalous dimension does not depend on all details of a scattering process, but only on the effective physics at the relevant scales. Based on that physical intuition we argue that the details of the regulator does not alter the singularity at the cusp, i.e. the divergent part. A similar argument was made in [30] in the context of the cusp anomalous dimension, where an exponential suppression factor was introduced to cut off the infrared, without modifying the cusp singularity. In momentum space, this corresponds to considering the Wilson lines slightly off-shell. A concern may be that this procedure breaks gauge invariance. This is indeed the case for the finite parts, but the gauge invariance is expected to be recovered for the divergent part. In the context of multiparton webs, such a suppression factor is also used [42].

In dimensional regularization, Wilson-line correlators do not depend on a physical scale. In reference [42], the soft function is regularized by introducing offshellness regulators δ_i on each Wilson line, which cut off the infrared (IR) divergences,

$$\mathcal{S}_{\delta_1, \dots, \delta_n} \equiv \langle 0 | \prod_i Y_{i, \delta_i} | 0 \rangle, \quad Y_{i, \delta_i} \equiv \mathbf{P}_{\delta_i} \exp \left[ig \int_0^\infty ds v_i \cdot A^a(sv_i) T^a \right], \quad (2.13)$$

where the modified path-ordered exponential reads

$$\begin{aligned} \mathbf{P}_\delta \exp \left[\int ds \right] &\equiv 1 + \int ds \theta(s) e^{i\delta s} + \frac{1}{2!} \iint ds_1 ds_2 \theta(s_1) \theta(s_2 - s_1) e^{i\delta s_2} \\ &\quad + \frac{1}{2!} \iint ds_1 ds_2 \theta(s_2) \theta(s_1 - s_2) e^{i\delta s_1} + \dots \end{aligned} \quad (2.14)$$

The modified soft function contains only UV ϵ -poles, which can be collected into a multiplicative renormalization \mathcal{Z} -factor for the Wilson-line operator such that

$$\mathcal{S}_{\delta_1, \dots, \delta_n}(v_i, \delta_i; \alpha_s; \epsilon) = \mathcal{S}_{\delta_1, \dots, \delta_n}^{\text{fin.}}(v_i, \delta_i/\delta_n, \mu/\delta_n; \alpha_s(\mu); \epsilon) \mathcal{Z}_n^{-1}(v_i; \alpha_s(\mu); \epsilon), \quad (2.15)$$

where $\mathcal{S}^{\text{fin.}}$ is finite at $\epsilon = 0$. The factor \mathcal{Z}_n is a matrix in color space satisfying the evolution equation [1, 5, 37, 38]

$$\frac{d}{d \ln \mu} \mathcal{Z}_n = -\mathcal{Z}_n \mathbf{\Gamma}_n. \quad (2.16)$$

In this way the soft anomalous dimension matrix can be determined order-by-order in α_s by extracting the UV ϵ -poles of the modified corrector $\mathcal{S}_{\delta_1, \dots, \delta_n}$.

The matrix \mathcal{Z}_n encodes the UV divergences and is therefore expected to be independent of the choice of IR regulators. We have the freedom to set the parameters δ_i to be any nonzero value. The standard choice is to consider $\mathcal{S}_{1, \dots, 1}$ where all δ_i 's are set to 1, see e.g. [11]. In the present work we adopt a new approach where we set all but one of them to be zero. In other words, we introduce the regulator on the last external leg only. Physically, one may think of that regulator arising from the emission of a photon or gluon. The latter provides an offshellness which regulates the infrared, while leaving the ultraviolet physics unchanged. Of course, introducing an ad-hoc regulator does not preserve gauge invariance in general, but — as in similar approaches in the literature — gauge invariance is expected

to be recovered for the soft anomalous dimension matrix. At the technical level, the novel regularization prescriptions leads to simpler HQET integrals.

In the following we explain how to apply the new method to determine the soft anomalous dimension matrix. For simplicity we focus on the three-line case where we consider $\mathcal{S}_{0,0,1}$ in the $\overline{\text{MS}}$ scheme.

Let us argue that $\mathcal{S}_{0,0,1}$ has the same ϵ -pole structures as the ratio between the standard three-line and two-line correlators, i.e. $[\mathcal{S}_{1,1}]^{-1}\mathcal{S}_{1,1,1}$, which implies that the finite remainder $\mathcal{S}_{0,0,1}^{\text{fin.}}(v_i, \mu; \alpha_s(\mu))$ obeys

$$\left[\mu \frac{\partial}{\partial \mu} + \beta(\alpha_s) \frac{\partial}{\partial \alpha_s} \right] \mathcal{S}_{0,0,1}^{\text{fin.}} = \Gamma_2 \mathcal{S}_{0,0,1}^{\text{fin.}} - \mathcal{S}_{0,0,1}^{\text{fin.}} \Gamma_3. \quad (2.17)$$

To see why the statement is true, it is helpful to introduce modified correlators $\mathcal{S}_{\delta,\delta}$ and $\mathcal{S}_{\delta,\delta,1}$ where $\delta \ll 1$. Let us consider the ratio $[\mathcal{S}_{\delta,\delta}(v_1, v_2)]^{-1}\mathcal{S}_{\delta,\delta,1}(v_1, v_2, v_3)$. Since the parameter δ is an IR cutoff, which characterizes the virtuality of the heavy particle $p^2 - m^2 \simeq m\delta$, the infrared singularity in $\mathcal{S}_{\delta,\delta,1}$, as δ goes to zero, factorizes and cancels with the two-line correlator. Therefore the ratio $[\mathcal{S}_{\delta,\delta}]^{-1}\mathcal{S}_{\delta,\delta,1}$ is regular in the $\delta \rightarrow 0$ limit at fixed order in α_s . Formally we can take the limit $\delta \rightarrow 0$ in this ratio, yielding

$$\lim_{\delta \rightarrow 0} [\mathcal{S}_{\delta,\delta}]^{-1}\mathcal{S}_{\delta,\delta,1} = [\mathcal{S}_{0,0}]^{-1}\mathcal{S}_{0,0,1} = \mathcal{S}_{0,0,1}, \quad (2.18)$$

where we set the scaleless function $\mathcal{S}_{0,0} = 1$. Our argument is based on expected factorization properties, a rigorous proof however is beyond the scope of this paper. In appendix A we explicitly verify relation (2.18) at the two-loop order, by carrying out an expansion by region analysis.

Likewise,

$$\lim_{\delta \rightarrow 0} [\mathcal{S}_{\delta,\delta}^{\text{fin.}}]^{-1}\mathcal{S}_{\delta,\delta,1}^{\text{fin.}} = \mathcal{S}_{0,0,1}^{\text{fin.}}. \quad (2.19)$$

Meanwhile, given the universal pole structure eq. (2.15), we have

$$[\mathcal{Z}_2]^{-1}[\mathcal{S}_{\delta,\delta}]^{-1}\mathcal{S}_{\delta,\delta,1}\mathcal{Z}_3 = [\mathcal{S}_{\delta,\delta}^{\text{fin.}}]^{-1}\mathcal{S}_{\delta,\delta,1}^{\text{fin.}}. \quad (2.20)$$

Taking the $\delta \rightarrow 0$ limit on both sides we find

$$\mathcal{Z}_2^{-1}\mathcal{S}_{0,0,1}\mathcal{Z}_3 = \mathcal{S}_{0,0,1}^{\text{fin.}}, \quad (2.21)$$

which is equivalent to the statement in eq. (2.17). Thus we observe, the ϵ -pole structure of the soft function $\mathcal{S}_{0,0,1}$ is governed by the ratio between \mathcal{Z}_3 and \mathcal{Z}_2 . This concludes our argument. Using Γ_2 , we can determine Γ_3 from $\mathcal{S}_{0,0,1}$ by demanding that the left-hand side of (2.21) is finite.

The procedure works with any number of Wilson lines at any loop order, as we demonstrate presently. Indeed, writing $\Gamma_n = \sum_{i=1}^{\infty} \alpha_s^i \Gamma_n^{(i)}$, and solving the renormalization group

equation (2.16) gives

$$\begin{aligned}
 \log \mathcal{Z}_n &= \alpha_s \frac{\Gamma_n^{(1)}}{2\epsilon} + \alpha_s^2 \left(\frac{\Gamma_n^{(2)}}{4\epsilon} - \frac{b_0}{4\epsilon^2} \Gamma_n^{(1)} \right) \\
 &+ \alpha_s^3 \left(\frac{\Gamma_n^{(3)}}{6\epsilon} + \frac{1}{48\epsilon^2} [\Gamma_n^{(1)}, \Gamma_n^{(2)}] - \frac{1}{6\epsilon^2} (b_0 \Gamma_n^{(2)} + b_1 \Gamma_n^{(1)}) + \frac{b_0^2}{6\epsilon^3} \Gamma_n^{(1)} \right) \\
 &+ \alpha_s^4 \left(\frac{\Gamma_n^{(4)}}{8\epsilon} + \frac{1}{48\epsilon^2} [\Gamma_n^{(1)}, \Gamma_n^{(3)}] - \frac{b_0}{8\epsilon^2} \Gamma_n^{(3)} + \frac{\Gamma_n^{(2)}}{8\epsilon^2} \left(\frac{b_0^2}{\epsilon} - b_1 \right) \right. \\
 &\quad \left. - \frac{\Gamma_n^{(1)}}{8\epsilon^2} \left(\frac{b_0^3}{\epsilon^2} - \frac{2b_0 b_1}{\epsilon} + b_2 \right) - \frac{b_0}{48\epsilon^3} [\Gamma_n^{(1)}, \Gamma_n^{(2)}] \right).
 \end{aligned} \tag{2.22}$$

Next, we write

$$\mathcal{S}_{0,\dots,0,\delta} = \exp \left(\sum_i \alpha_s^i w_n^{(i)} \right) = \exp \left(\sum_{i,j} \alpha_s^i \epsilon^j w_n^{(i,j)} \right), \tag{2.23}$$

where $w_n^{(i)}$ is the coefficient of α_s^i in the exponent and $w_n^{(i,j)}$ is the coefficient of $\alpha_s^i \epsilon^j$. We have also reinstated an arbitrary regulator δ . We then impose $\mathcal{Z}_{n-1}^{-1} \mathcal{S}_n \mathcal{Z}_n = \text{finite}$, at each order in the coupling constant. At the first order this implies the relation

$$\Gamma_n^{(1)} = \Gamma_{n-1}^{(1)} - 2w_n^{(1,-1)}. \tag{2.24}$$

Hence we obtain $\Gamma_n^{(1)}$ from $\Gamma_{n-1}^{(1)}$, supplemented by $w_n^{(1,-1)}$. Proceeding to the next orders, we have

$$\Gamma_n^{(2)} = \Gamma_{n-1}^{(2)} - 4w_n^{(2,-1)} + 2 [\Gamma_{n-1}^{(1)}, w_n^{(1,0)}] - 2 [w_n^{(1,-1)}, w_n^{(1,0)}], \tag{2.25}$$

$$\begin{aligned}
 \Gamma_n^{(3)} &= \Gamma_{n-1}^{(3)} - 6w_n^{(3,-1)} + \frac{3}{2} b_0 [w_n^{(1,-1)}, w_n^{(1,1)}] + 3 [w_n^{(1,0)}, w_n^{(2,-1)}] \\
 &+ 3 [w_n^{(2,0)}, w_n^{(1,-1)}] + [w_n^{(1,0)}, [w_n^{(1,-1)}, w_n^{(1,0)}]] - [w_n^{(1,-1)}, [w_n^{(1,-1)}, w_n^{(1,1)}]] \\
 &+ \frac{3}{2} [\Gamma_{n-1}^{(2)}, w_n^{(1,0)}] - \frac{3}{2} b_0 [\Gamma_{n-1}^{(1)}, w_n^{(1,1)}] \\
 &+ \frac{3}{4} [\Gamma_{n-1}^{(1)}, [w_n^{(1,-1)}, w_n^{(1,1)}]] + \frac{3}{4} [w_n^{(1,-1)}, [\Gamma_{n-1}^{(1)}, w_n^{(1,1)}]] + 3 [\Gamma_{n-1}^{(1)}, w_n^{(2,0)}] \\
 &- \frac{3}{4} [\Gamma_{n-1}^{(1)}, [\Gamma_{n-1}^{(1)}, w_n^{(1,1)}]] + \frac{3}{2} [w_n^{(1,0)}, [w_n^{(1,0)}, \Gamma_{n-1}^{(1)}]].
 \end{aligned} \tag{2.26}$$

Eqs. (2.24), (2.25) and (2.26) specify all the ingredients needed to determine the soft anomalous dimension matrix up to three-loop order. Requiring higher-order poles to cancel implies further relations. For instance we have

$$w_n^{(2,-2)} = \frac{1}{4} [\Gamma_{n-1}^{(1)}, w_n^{(1,-1)}]. \tag{2.27}$$

This can be used as a consistency check when calculating the two-loop web function $w_n^{(2)}$.

We will demonstrate in the following section that eq. (2.25) reproduces the correct two-loop result for $\Gamma_3^{(2)}$.

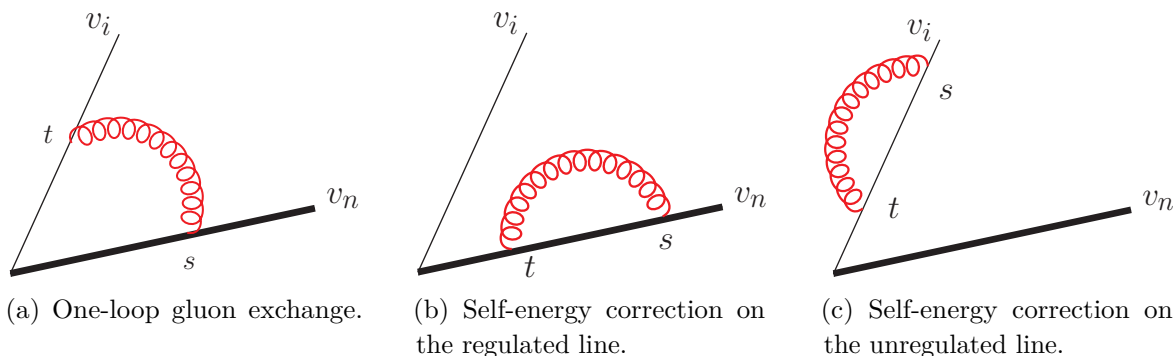


Figure 1. The three one-loop diagrams.

3 The two-loop soft anomalous dimension matrix via the new method

3.1 One loop

The one-loop soft anomalous dimension can be found from the recurrence equation in eq. (2.24). Solving eq. (2.24) we find

$$\Gamma_n^{(1)} = -2 \sum_{i=1}^n w_i^{(1,-1)}, \quad (3.1)$$

where $w_i^{(1,-1)}$ is the single pole of the soft function that involves Wilson lines 1 to i , in eq. (2.23). We recall that only the n -th Wilson line is IR-regulated.

There are two contributions to $w_n^{(1)}$: firstly, a gluon exchange between the regulated n -th Wilson line and an unregulated i -th line, with $i = \{0, \dots, n-1\}$, and secondly, the self-energy (SE) graph involving the n -th Wilson line. The former is shown in figure 1(a), whereas the latter in figure 1(b). Other potential contributions, due to gluon exchanges involving unregulated lines only, vanish as the integrals are scaleless. For example, the self-energy on an unregulated line is shown in figure 1(c). Note that this involves a cancellation between the IR and the UV.

It is convenient to compute the one-loop exchanges in configuration space where the Feynman-gauge gluon propagator is given by

$$\int \frac{d^d k}{(2\pi)^d} \frac{e^{-ik \cdot x} (-ig_{\mu\nu})}{k^2 + i\varepsilon} = -\frac{\Gamma(1-\epsilon)}{4\pi^{2-\epsilon}} \frac{g_{\mu\nu}}{(-x^2 + i\varepsilon)^{1-\epsilon}}, \quad (3.2)$$

and where x is the spacetime distance associated to the gluon propagator. In the diagram shown in figure 1(a), it is given by $x = sv_n - tv_i$. Here s, t are line parameters that are integrated along the semi-infinite Wilson line segments, i.e. $s, t \in [0, \infty]$. In figure 1(b) we have $t \in [0, s]$ and $s \in [0, \infty]$.

We write the total contribution to $w_n^{(1)}$ as

$$\alpha_s w_n^{(1)} = g_s^2 \mu^{2\epsilon} \frac{\Gamma(1-\epsilon)}{4\pi^{2-\epsilon}} \left[\sum_{i=1}^{n-1} \mathbf{T}_i \cdot \mathbf{T}_n v_i \cdot v_n \int_0^\infty ds dt \frac{e^{i\delta s}}{(-(sv_n - tv_i)^2 + i\varepsilon)^{1-\epsilon}} + \frac{C_n}{2} \int_0^\infty ds e^{i\delta s} \int_0^s dt \frac{1}{(-(sv_n - tv_n)^2 + i\varepsilon)^{1-\epsilon}} \right], \quad (3.3)$$

where $C_i = \mathbf{T}_i^a \mathbf{T}_i^a$ is the quadratic Casimir associated to line i . The integrals in eq. (3.3) can be performed to all orders in ϵ , resulting in a ${}_2F_1$ function. However, we will only require the expansion in ϵ . In order to display the results, it is convenient to define the integral $f(x, \epsilon)$ and its expansion in ϵ as follows

$$f(x, \epsilon) = -\frac{1}{2} \left(x + \frac{1}{x} \right) \int_0^\infty dt \frac{1}{(t + \frac{1}{x})^{1-\epsilon} (t+x)^{1-\epsilon}} = \frac{r(x)}{2} \sum_{n=0}^\infty \frac{\epsilon^n}{n!} M_{n00}(x), \quad (3.4a)$$

$$r(x) = \frac{1+x^2}{1-x^2}, \quad (3.4b)$$

$$M_{000}(x) = 2 \log(x), \quad (3.4c)$$

$$M_{100}(x) = 2 \text{Li}_2(x^2) + 4 \log(x) \log(1-x^2) - 2 \log^2(x) - 2\zeta_2. \quad (3.4d)$$

The functions M_{n00} are a subset of a larger class of functions M_{klm} which form a basis of functions for multiple-gluon exchange webs [44], where three- and four-gluon vertices are absent. We only display the explicit results up to M_{100} as this is all we require to two loops. The one-loop web contribution in eq. (3.3) can be written as

$$\alpha_s w_n^{(1)} = -\frac{\alpha_s}{\pi} \left(\frac{\mu^2}{\delta^2} \right)^\epsilon \frac{\Gamma(1-\epsilon)}{\pi^{-\epsilon}} \left[\sum_{i=1}^{n-1} \mathbf{T}_i \cdot \mathbf{T}_n f(x_{in}, \epsilon) \Gamma(2\epsilon) + \frac{C_n}{2} \Gamma(-1+2\epsilon) \right] \quad (3.5)$$

$$= -\frac{\alpha_s}{\pi} \left(\frac{\bar{\mu}^2}{\bar{\delta}^2} \right)^\epsilon e^{\epsilon\gamma_E} \Gamma(1-\epsilon) \left[\sum_{i=1}^{n-1} \mathbf{T}_i \cdot \mathbf{T}_n f(x_{in}, \epsilon) \Gamma(2\epsilon) + \frac{C_n}{2} \Gamma(-1+2\epsilon) \right], \quad (3.6)$$

where $\bar{\mu}^2 = 4\pi e^{-\gamma_E} \mu^2$ is the $\overline{\text{MS}}$ scale, $\bar{\delta} = 2\delta$ is a modified regulator and we have used the convenient x_{ij} variables defined in eq. (2.6). The coefficients as an expansion in ϵ are then

$$\alpha_s w_n^{(1,-1)} = -\frac{\alpha_s}{4\pi} \left[\sum_{i=1}^{n-1} \mathbf{T}_i \cdot \mathbf{T}_n r(x_{in}) M_{000}(x_{in}) - C_n \right], \quad (3.7)$$

$$\begin{aligned} \alpha_s w_n^{(1,0)} &= -\frac{\alpha_s}{4\pi} \left[\sum_{i=1}^{n-1} \mathbf{T}_i \cdot \mathbf{T}_n r(x_{in}) M_{100}(x_{in}) - 2 C_n \right] \\ &\quad - \frac{\alpha_s}{4\pi} \log \left(\frac{\bar{\mu}^2}{\bar{\delta}^2} \right) \left[\sum_{i=1}^{n-1} \mathbf{T}_i \cdot \mathbf{T}_n r(x_{in}) M_{000}(x_{in}) - C_n \right]. \end{aligned} \quad (3.8)$$

Then using eq. (3.7) in eq. (3.1), we have the result for the one-loop anomalous dimension

$$\alpha_s \Gamma_n^{(1)} = \frac{\alpha_s}{2\pi} \sum_{i=1}^n \left[\sum_{j=1}^{i-1} \mathbf{T}_i \cdot \mathbf{T}_j r(x_{ij}) M_{000}(x_{ij}) - C_i \right]. \quad (3.9)$$

Eq. (3.9) is in agreement with the classic result of Korchemsky and Radyushkin [45]. In our computation of $\Gamma_n^{(1)}$, we have had to handle conceptual issues around extra infrared poles, as correlations between unregulated Wilson lines vanish. These are then accounted for in eq. (3.1) by effectively adding them back. We will see in the remaining sections that using our regularisation scheme is combinatorically more complex than when all the lines are regulated due to a lack of symmetry. However, the integrals become simpler and can be computed using standard methods, as only one line is regulated.

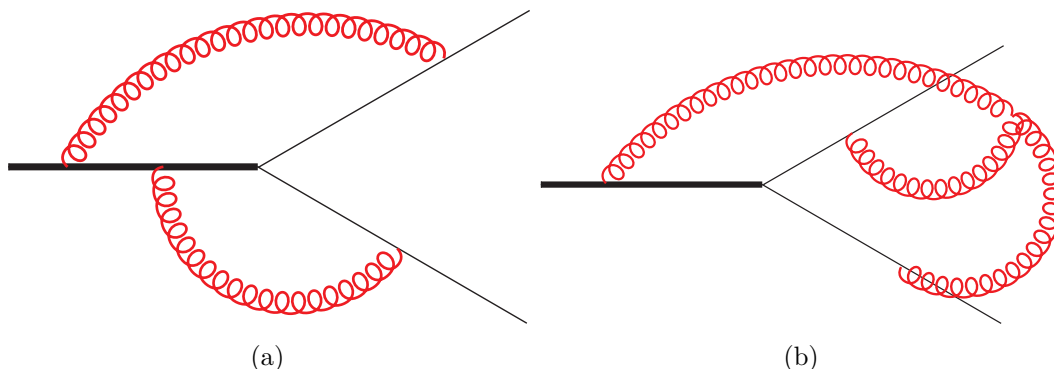


Figure 2. Contributions to the two-loop soft anomalous dimension matrix.

3.2 Two loops

The two-loop contribution to the soft anomalous dimension is described by eq. (2.25). In this section we compute it for the case of three Wilson lines, focusing on structures connecting all three lines, cf. eq. (2.10). In this case, we do not have the first term of eq. (2.25), $\Gamma_2^{(2)}$, and we do not consider any two-particle colour structures. Thus we write

$$\Gamma_3^{(2)} \Big|_{\text{connected}} = \left\{ -4w_3^{(2,-1)} + 2 \left[\Gamma_2^{(1)}, w_3^{(1,0)} \right] - 2 \left[w_3^{(1,-1)}, w_3^{(1,0)} \right] \right\} \Big|_{\text{connected}}. \quad (3.10)$$

At two loops, there are two types of graphs connecting all three lines. One of them is the gluon exchange diagram shown in figure 2(a), which we label as [1, 2, 1]. (This notation keeps track of the number of gluon attachments to each line.) The other graph is the three-gluon-vertex diagram shown in figure 2(b). The calculation of these graphs is instructive. The calculation of the gluon exchange diagram shows us how to deal with a subtlety related to infrared divergences, while that of the three-gluon-vertex diagram shows us the computational advantages of regulating only one Wilson line.

3.2.1 Gluon exchange diagram

For the case of the [1, 2, 1], the contributions to $w_3^{(2,-1)}$ in eq. (3.10) are shown in figure 3. The diagrams correspond to each permutation of gluon attachments to the Wilson lines. The thick Wilson line, v_3 is the regulated one. Diagrams 3(f) and 3(e) can be obtained from diagrams 3(a) and 3(b), respectively, by interchanging v_1 and v_2 . Therefore, we only need to compute diagrams 3(a)–(d).

Diagrams 3(a) and 3(b) have the kinematic factor

$$F_{3(a)} - F_{3(b)} = (v_1 \cdot v_2)(v_2 \cdot v_3) \int_0^\infty du dt_1 dt_2 ds e^{i\delta s} \frac{\theta(t_1 - t_2) - \theta(t_2 - t_1)}{(-(sv_3 - t_1 v_2)^2)^{1-\epsilon} (-(uv_1 - t_2 v_2)^2)^{1-\epsilon}}, \quad (3.11)$$

whereas diagrams 3(c) and 3(d) are

$$F_{3(c)} - F_{3(d)} = (v_1 \cdot v_3)(v_2 \cdot v_3) \int_0^\infty du dt ds_1 ds_2 \frac{e^{i\delta s_1} \theta(s_1 - s_2) - e^{i\delta s_2} \theta(s_2 - s_1)}{(-(s_1 v_3 - uv_1)^2)^{1-\epsilon} (-(s_2 v_3 - tv_2)^2)^{1-\epsilon}}, \quad (3.12)$$

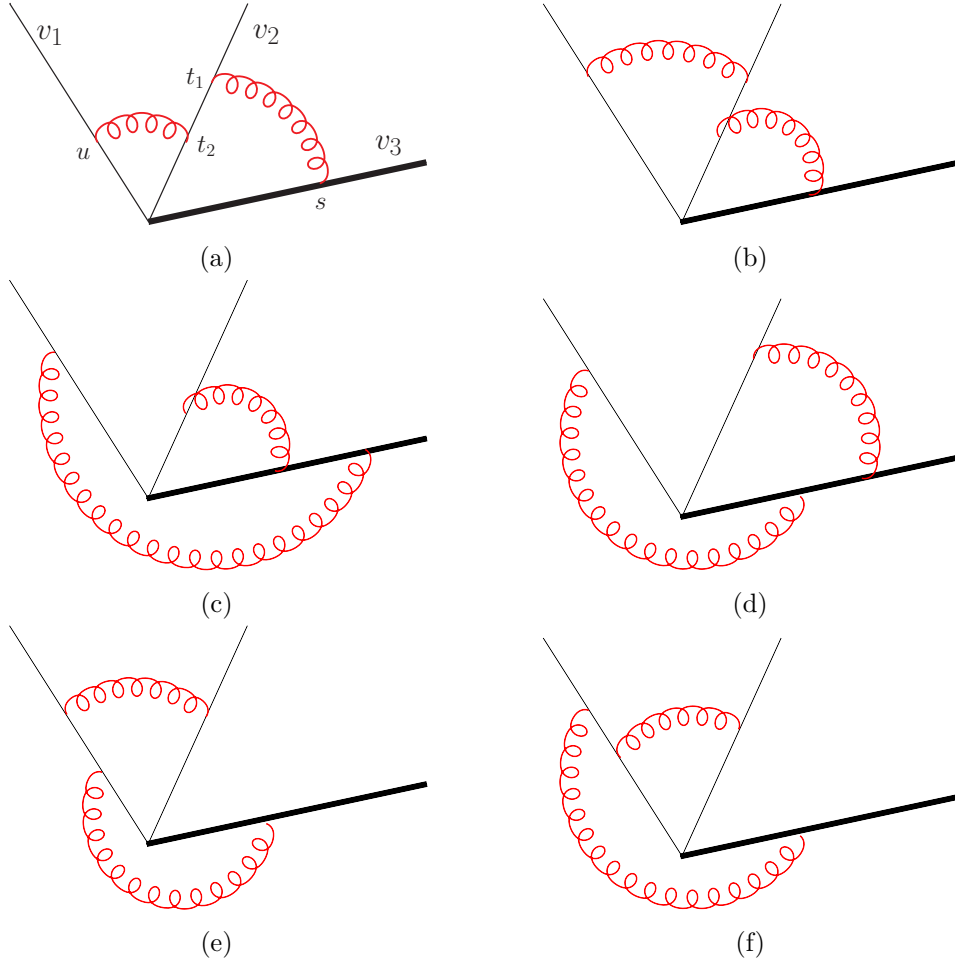


Figure 3. Two-loop gluon exchange diagrams contributing to three-line color structures.

where the relative minus signs comes from non-Abelian exponentiation. It is reminded that the exponential damping factor $e^{i\delta s}$ is only added to the outer most attachment on v_3 . The contribution to $w_3^{(2)}$ is

$$w_{3,[1,2,1]}^{(2)} = \frac{\mathcal{T}_{123}}{2\pi^2} \left[(F_{3(a)} - F_{3(b)}) - (F_{3(a)} - F_{3(b)})(v_1 \leftrightarrow v_2) + F_{3(c)} - F_{3(d)} \right]. \quad (3.13)$$

Here we denoted the overall triple colour factor by $\mathcal{T}_{123} \equiv if^{abc}\mathbf{T}_1^a\mathbf{T}_2^b\mathbf{T}_3^c$. The combination $F_{3(a)} - F_{3(b)}$ can be computed to give

$$F_{3(a)} - F_{3(b)} = e^{-4\epsilon\gamma_E}(\delta^2)^{-2\epsilon} \frac{r(x_{12})r(x_{23})}{16} \left[\frac{1}{\epsilon^2} M_{000}(x_{12})M_{000}(x_{23}) + \frac{1}{\epsilon} (M_{000}(x_{12})M_{100}(x_{23}) + M_{100}(x_{12})M_{000}(x_{23})) \right], \quad (3.14)$$

whereas

$$F_{3(c)} - F_{3(d)} = 0, \quad (3.15)$$

due to symmetry. We define a modified M_{100} function to absorb regulator-dependent terms as follows,

$$M_{100}^{(\kappa)}(x) = M_{100}(x) + \log(e^{-\kappa\gamma_E} \delta^{-2\kappa}) M_{000}(x). \quad (3.16)$$

Using $w^{(1,-1)}$ from eq. (3.7), $w^{(1,0)}$ from eq. (3.8) and $\Gamma_2^{(1)}$ from eq. (3.9), the three contributions to eq. (3.10) are then written as

$$\begin{aligned} -4 w_{3,[1,2,1]}^{(2,-1)} &= \frac{\mathcal{T}_{123}}{8\pi^2} r(x_{12}) \left\{ r(x_{13}) \left[M_{100}(x_{12}) M_{000}(x_{13}) + M_{000}(x_{12}) M_{100}^{(2)}(x_{13}) \right] \right. \\ &\quad \left. - r(x_{23}) \left[M_{100}(x_{12}) M_{000}(x_{23}) + M_{000}(x_{12}) M_{100}^{(2)}(x_{23}) \right] \right\}, \\ 2 \left[\Gamma_2^{(1)}, w_3^{(1,0)} \right] &= \frac{\mathcal{T}_{123}}{4\pi^2} r(x_{12}) M_{000}(x_{12}) \left[r(x_{23}) M_{100}^{(1)}(x_{23}) - r(x_{13}) M_{100}^{(1)}(x_{13}) \right], \\ -2 \left[w_3^{(1,-1)}, w_3^{(1,0)} \right] &= \frac{\mathcal{T}_{123}}{8\pi^2} r(x_{13}) r(x_{23}) \left[M_{100}^{(1)}(x_{13}) M_{000}(x_{23}) - M_{000}(x_{13}) M_{100}^{(1)}(x_{23}) \right]. \end{aligned} \quad (3.17)$$

The sum of the above gives

$$\Gamma_{3,[1,2,1]}^{(2)} = \mathcal{T}_{123} \left(\frac{1}{8\pi^2} \right) \sum_{i,j,k} \varepsilon_{ijk} r(x_{ij}) r(x_{ik}) M_{100}(x_{ij}) M_{000}(x_{ik}), \quad (3.18)$$

where all the dependence on the regulator δ cancels, as expected.

3.2.2 The three-gluon-vertex diagram

To complete the calculation of the three-line soft anomalous dimension at two loops we require the coefficient of the single pole of figure 2(b). Using our new method that places a regulator only on one Wilson line, we find that only four basis integrals are required in the top sector, as opposed to six in the traditional approach [23, 24]. (See also [46] for a calculation using unitarity cuts.)

The contribution to the exponent of the soft function is written as

$$\begin{aligned} w_{3,3gv}^{(2)} &= \frac{\mathcal{T}_{123}}{16\pi^2} (\bar{\mu}^2)^{2\epsilon} e^{2\epsilon\gamma_E} \\ &\quad \times \int \frac{d^d k_1}{i\pi^{d/2}} \frac{d^d k_2}{i\pi^{d/2}} \int d^d k_3 \frac{\delta^{(d)}(k_1 + k_2 + k_3) \sum_{i,j,k} \epsilon_{ijk} (v_i \cdot v_j) (k_i \cdot v_k)}{k_1^2 k_2^2 (k_1 + k_2)^2 (k_1 \cdot v_1) (k_2 \cdot v_2) (k_3 \cdot v_3 - \delta)}. \end{aligned} \quad (3.19)$$

We will conveniently set $\delta = 1$ as the dependence on δ can be easily recovered by counting mass dimensions. We define the integral family as

$$\begin{aligned} I_{a_1 a_2 a_3 a_4 a_5 a_6 a_7 a_8 a_9}^{[3gv]} &= e^{2\epsilon\gamma_E} \int \frac{d^d k_1}{i\pi^{d/2}} \frac{d^d k_2}{i\pi^{d/2}} \\ &\quad \times \frac{(k_1 \cdot v_2)^{-a_7} (k_2 \cdot v_3)^{-a_8} (k_2 \cdot v_1)^{-a_9}}{(k_1^2)^{a_1} (k_2^2)^{a_2} ((k_1 + k_2)^2)^{a_3} (k_1 \cdot v_1)^{a_4} (k_2 \cdot v_2)^{a_5} (-(k_1 + k_2) \cdot v_3 - 1)^{a_6}}. \end{aligned} \quad (3.20)$$

Using Kira [47] we identify 16 basis integrals, 4 of which are in the top sector $I_{111111000}^{[3gv]}$. Differential equations are derived with respect to the three x_{ij} variables. The rotation to canonical form [22] is found using a combination of techniques. For the lower sectors, using

the automated package `CANONICA` [48], is enough. For the top sector we use `DlogBasis` [49] to reveal uniform weight integrals. Through this method we find the following three integrals,

$$g_{13}^{[3gv]} = \epsilon^4 \frac{1 - x_{13}^2}{x_{13}} I_{1111111-100}^{[3gv]}, \quad (3.21a)$$

$$g_{14}^{[3gv]} = \epsilon^4 \frac{1 - x_{12}^2}{x_{12}} I_{11111110-10}^{[3gv]}, \quad (3.21b)$$

$$g_{15}^{[3gv]} = \epsilon^4 \frac{1 - x_{23}^2}{x_{23}} I_{111111100-1}^{[3gv]}. \quad (3.21c)$$

The last required integral is found using `INITIAL` [50]

$$g_{16}^{[3gv]} = \epsilon^3 \left(2I_{1111112-10-1}^{[3gv]} + (v_1 \cdot v_3) I_{1111112-100}^{[3gv]} + (v_2 \cdot v_3) I_{111111200-1}^{[3gv]} \right) + \text{lower sectors}. \quad (3.22)$$

Using this integral basis, we find a differential equation in the canonical form [22]

$$d\mathbf{g}^{[3gv]} = \epsilon \sum_{\ell \in \mathcal{A}^{[3gv]}} c_\ell^{[3gv]} d \log(\ell) \mathbf{g}^{[3gv]}, \quad (3.23)$$

where the set of ℓ , the alphabet \mathcal{A} , is

$$\begin{aligned} \mathcal{A}^{[3gv]} = \{ & 1 - x_{12}, x_{12}, 1 + x_{12}, 1 - x_{13}, x_{13}, 1 + x_{13}, 1 - x_{23}, x_{23}, 1 + x_{23}, \\ & x_{12}x_{13} + x_{23}, x_{12}x_{23} + x_{13}, x_{12} + x_{13}x_{23}, 1 + x_{12}x_{13}x_{23} \}. \end{aligned} \quad (3.24)$$

To solve the system in eq. (3.23) we need a boundary condition. We choose $x_{ij} = 1$ for all i and j . At this boundary point, the lower sector integrals are just iterated eikonal bubbles which evaluate to

$$\int \frac{d^d k}{i\pi^{d/2}} \frac{1}{(k^2)^\alpha (k \cdot v - 1)^\beta} = (-1)^{\alpha+\beta} \frac{2^{d-2\alpha} \Gamma(d/2 - \alpha) \Gamma(2\alpha + \beta - d)}{\Gamma(\alpha) \Gamma(\beta)}, \quad (3.25)$$

or, because of the differing regulators on different lines,

$$\begin{aligned} \int \frac{d^d k}{i\pi^{d/2}} \frac{1}{(k^2)^\alpha (k \cdot v - 1)^\beta (k \cdot v)^\gamma} \\ = (-1)^{\alpha+\beta+\gamma} \frac{2^{d-2\alpha} \Gamma(d/2 - \alpha) \Gamma(d - 2\alpha - \gamma) \Gamma(2\alpha + \beta + \gamma - d)}{\Gamma(\alpha) \Gamma(\beta) \Gamma(d - 2\alpha)}. \end{aligned} \quad (3.26)$$

The top sector integrals $g_{13}^{[3gv]}$ to $g_{15}^{[3gv]}$ in eqs. (3.21a)–(3.21c) clearly vanish at such a boundary. However, $g_{16}^{[3gv]}$ in eq. (3.22) does not and depends on integrals more complicated than the bubble integrals in eqs. (3.25) and (3.26). Instead of attempting to compute them or determining from physical consistency conditions obtained from the differential equations (see e.g. [49]), we will fix the remaining boundary value from knowledge of the lightlike limit.

Solving the differential equation gives the following expansion in ϵ for $w_{3,3gv}^{(2)}$ in eq. (3.19)

$$w_{3,3gv}^{(2,-3)} = \mathcal{T}_{123} \frac{c_0}{16\pi^2} (r(x_{13})M_{000}(x_{13}) - r(x_{23})M_{000}(x_{23})) \quad (3.27a)$$

$$w_{3,3gv}^{(2,-2)} = \mathcal{T}_{123} \frac{c_1}{16\pi^2} (r(x_{13})M_{000}(x_{13}) - r(x_{23})M_{000}(x_{23})) \quad (3.27b)$$

$$\begin{aligned} w_{3,3gv}^{(2,-1)} = \frac{\mathcal{T}_{123}}{32\pi^2} \left\{ \frac{1}{2} \sum_{ijk} \epsilon_{ijk} r(x_{ij}) M_{000}(x_{ij}) M_{000}(x_{ik})^2 \right. \\ \left. - c_2 [r(x_{13})M_{000}(x_{13}) - r(x_{23})M_{000}(x_{23})] \right\}, \end{aligned} \quad (3.27c)$$

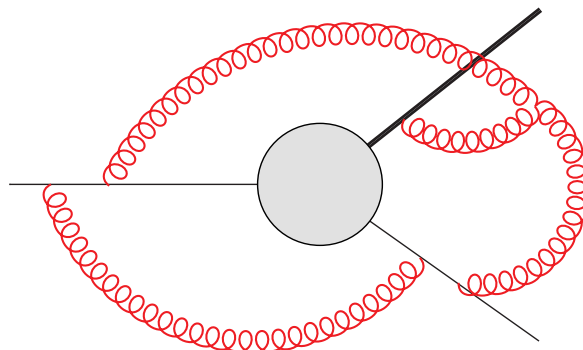


Figure 4. The three-loop $w_{122}^{(3)}$ diagram.

where the c_i are constants coming from the remaining integral and the subscript denotes its transcendental weight. The web only has a single pole divergence, thus $c_0 = c_1 = 0$. Together with eq. (3.18) the complete three-line two-loop soft anomalous dimension is

$$\Gamma_3^{(2)} = -\mathcal{T}_{123} \frac{1}{8\pi^2} \left\{ \sum_{ijk} \epsilon_{ijk} r(x_{ij}) M_{000}(x_{ij}) \left(r(x_{ik}) M_{100}(x_{ik}) + \frac{1}{2} M_{000}(x_{ik})^2 \right) - c_2 \left(r(x_{13}) M_{000}(x_{13}) - r(x_{23}) M_{000}(x_{23}) \right) \right\}. \quad (3.28)$$

In the lightlike limit, when all $x_{ij} \rightarrow 0$ simultaneously, we have

$$\lim_{x_{ij} \rightarrow 0} \Gamma_3^{(2)} = \mathcal{T}_{123} \frac{c_2}{4\pi^2} \log \frac{x_{13}}{x_{23}}. \quad (3.29)$$

It is known that there is no tripole colour structure when all Wilson lines are lightlike, since we cannot construct conformally invariant cross ratios [51]. Therefore we conclude that $c_2 = 0$, giving

$$\Gamma_3^{(2)} = -\mathcal{T}_{123} \frac{1}{8\pi^2} \sum_{ijk} \epsilon_{ijk} r(x_{ij}) M_{000}(x_{ij}) \left(r(x_{ik}) M_{100}(x_{ik}) + \frac{1}{2} M_{000}(x_{ik})^2 \right), \quad (3.30)$$

in agreement with previous computations [13–16].

In summary, we see that the calculation of the two-loop soft anomalous dimension matrix is greatly simplified by regulating only one of the multiple Wilson lines. In the next section, we show that the new method is promising for higher-loop applications as well.

4 Three-loop calculation of a three-line web function

To illustrate the potential of the new method, we evaluate in this section a three-loop web diagram. This is a contribution to the soft anomalous dimension matrix of three Wilson lines at the three-loop order. Naturally, many further diagrams are required for the full calculation. Here, our intention is to provide a proof-of-concept by calculating a diagram, shown in figure 4, of genuine complexity.

The kinematic part of the integral shown in figure 4 can be conveniently written as

$$\mathcal{F}_{122}^{(3)} = \int \frac{d^d k_1}{i\pi^{d/2}} \frac{d^d k_2}{i\pi^{d/2}} \frac{d^d k_3}{i\pi^{d/2}} \quad (4.1)$$

$$\times \int d^d k_4 \frac{\delta^{(d)}(k_1 + k_2 + k_3) \sum_{i,j,k} \epsilon_{ijk} (v_i \cdot v_j)(v_k \cdot k_i)}{k_1^2 k_2^2 k_3^2 k_4^2 (k_1 \cdot v_1)((k_1 - k_4) \cdot v_1)(k_4 \cdot v_2)((k_2 + k_4) \cdot v_2)(k_3 \cdot v_3 - 1)}.$$

Using Kira [47] we find that there are 66 basis integrals, belonging to 22 sectors. The dimension of the sector with the most number of integrals is 8. We then find the differential equation satisfied by these integrals.

For the transformation of the differential equation to canonical form, we found it convenient to transform sector-by-sector. The diagonal block transformations were found using either CANONICA [48] or using DlogBasis [49] to identify one uniform weight integral and then using INITIAL [50] for the transformation.

Once all the diagonal blocks are in canonical form, we then need to transform all the off-diagonal blocks. For this we used a combination of CANONICA and Libra [52]. We write our equation as

$$d\mathbf{g}^{[122]} = \epsilon \sum_{\ell \in \mathcal{A}^{[122]}} c_\ell^{[122]} d\log(\ell) \mathbf{g}^{[122]}, \quad (4.2)$$

where $c_\ell^{[122]}$ are 66×66 constant matrices. The canonical differential equation matrices $c^{[122]}$, as well as the definition of the canonical basis $\mathbf{g}^{[122]}$, are included in the ancillary files. The alphabet appearing in the differential equation involves two additional letters compared to the two-loop case of eq. (3.24), namely

$$\{x_{13} + x_{12}x_{23} + x_{12}x_{13}^2x_{23} + x_{13}x_{23}^2, x_{12}x_{13} + x_{23} + x_{13}^2x_{23} + x_{12}x_{13}x_{23}^2\}. \quad (4.3)$$

In order to fully solve the differential equation we need a boundary condition. In practice, we consider kinematic points $v_i = v, v_j = v, v_k = -v$, where 36 of the 66 integrals can be found analytically. Either they vanish or reduce to real-valued iterated integrals of the form given in eqs. (3.25) and (3.26). This does not completely fix the required constants for the single pole of $\mathcal{F}_{122}^{(3)}$ which we label as $\mathcal{F}_{122}^{(3,-1)}$. We can find the remaining constants by imposing finiteness of the differential equation on single-variable slices. Consider the single-variable regime $(x_{12}, x_{13}, x_{23}) = (1, x, x)$. Then we impose the condition that eq. (4.2) remains finite as $x \rightarrow 1$ and $x \rightarrow \pm i$. Doing this also for the other permutations we find we can fix all the boundary conditions.

Thus we arrive at the result

$$\mathcal{F}_{122}^{(3,-1)} = r(x_{12})^2 f_A(x_{12}, x_{13}, x_{23}) + r(x_{12})r(x_{13})f_B(x_{12}, x_{13}, x_{23}) + r(x_{12})r(x_{23})f_C(x_{12}, x_{13}, x_{23}), \quad (4.4)$$

where the functions f_A, f_B and f_C are of pure weight five. They can be written in terms of classical polylogarithms $\text{Li}_n(-s)$ up to weight $n = 5$, with the following arguments,

$$s \in \left\{ x_{12}, -x_{12}, x_{13}, -x_{13}, \frac{x_{12}}{x_{13}x_{23}}, \frac{x_{12}x_{13}}{x_{23}}, \frac{x_{12}x_{23}}{x_{13}}, x_{12}x_{13}x_{23} \right\}. \quad (4.5)$$

Their symbols are drawn from a smaller set of alphabets given in eq. (3.24). The expressions for $f_{A,B,C}$ are given explicitly in the ancillary files.

We would like to present the total contribution of web function $w_{122}^{(3)}$ after symmetrization under permutations of Wilson lines. Hence let us introduce a basis $\{g_A^\pm, g_B^\pm, g_C^\pm\}$ defined as follows

$$\begin{aligned} g_A^\pm(3, 2, 1) &= \pm g_A^\pm(3, 1, 2) \equiv \frac{1}{2} [f_A(x_{12}, x_{13}, x_{23}) \pm (x_{13} \leftrightarrow x_{23})], \\ g_B^\pm(3, 2, 1) &= \pm g_B^\pm(2, 3, 1) \equiv \frac{1}{2} [f_B(x_{12}, x_{13}, x_{23}) \pm (x_{12} \leftrightarrow x_{13})], \\ g_C^\pm(3, 2, 1) &= \pm g_C^\pm(1, 2, 3) \equiv \frac{1}{2} [f_C(x_{12}, x_{13}, x_{23}) \pm (x_{12} \leftrightarrow x_{23})]. \end{aligned} \quad (4.6)$$

where we adopt a short-hand notation $g(i, j, k) = g(\alpha_i, \alpha_j, \alpha_k)$ where

$$\alpha_3 \equiv x_{12}, \quad \alpha_2 \equiv x_{13}, \quad \alpha_1 \equiv x_{23}. \quad (4.7)$$

In this notation the permutation among Wilson lines $v_{i,j,k}$ is equivalent to the permutation among arguments of the function $g(i, j, k)$.

Summing over all six permutations of the web diagram $\mathcal{F}_{122}^{(3)}$, we obtain

$$\begin{aligned} \mathcal{C}(1, 2, 3) \mathcal{F}_{122}^{(3)}(3, 2, 1) + \text{perm.} &= \frac{1}{\epsilon} \quad (4.8) \\ &\times \left\{ r(1)^2 \left([\mathcal{C}(3, 2, 1) + \mathcal{C}(2, 3, 1)] g_A^+(1, 2, 3) + [\mathcal{C}(3, 2, 1) - \mathcal{C}(2, 3, 1)] g_A^-(1, 2, 3) \right) \right. \\ &\quad + r(3)r(2) \left([\mathcal{C}(1, 2, 3) + \mathcal{C}(1, 3, 2)] g_B^+(3, 2, 1) + [\mathcal{C}(1, 2, 3) - \mathcal{C}(1, 3, 2)] g_B^-(3, 2, 1) \right. \\ &\quad \left. \left. + [\mathcal{C}(2, 1, 3) + \mathcal{C}(3, 1, 2)] g_C^+(3, 1, 2) + [\mathcal{C}(2, 1, 3) - \mathcal{C}(3, 1, 2)] g_C^-(3, 1, 2) \right) \right. \\ &\quad \left. + \text{cyc.} \right\}. \end{aligned}$$

The expression in the braces is manifestly symmetric under exchange $2 \leftrightarrow 3$, and cyc. represents the sum of two cyclic permutations. The color factor $\mathcal{C}(1, 2, 3) = \mathbf{T}_1^c [\mathbf{T}_3 \cdot \mathbf{T}_1, \mathbf{T}_3 \cdot \mathbf{T}_2] \mathbf{T}_2^c$ is associated with the diagram we computed, whose maximally non-abelian component can be decomposed onto the following basis,

$$\begin{aligned} &\mathbf{T}_1^c [\mathbf{T}_3 \cdot \mathbf{T}_1, \mathbf{T}_3 \cdot \mathbf{T}_2] \mathbf{T}_2^c - \frac{1}{2} \left\{ \mathbf{T}_1 \cdot \mathbf{T}_2, [\mathbf{T}_3 \cdot \mathbf{T}_1, \mathbf{T}_3 \cdot \mathbf{T}_2] \right\} \quad (4.9) \\ &= \frac{1}{4} [\mathbf{T}_3^a, \mathbf{T}_3^b] [\mathbf{T}_1^c, \mathbf{T}_1^a] \{ \mathbf{T}_2^b, \mathbf{T}_2^c \} + \frac{1}{4} [\mathbf{T}_3^a, \mathbf{T}_3^b] \{ \mathbf{T}_1^c, \mathbf{T}_1^a \} [\mathbf{T}_2^b, \mathbf{T}_2^c] + \frac{1}{2} [\mathbf{T}_3^a, \mathbf{T}_3^b] [\mathbf{T}_1^c, \mathbf{T}_1^a] [\mathbf{T}_2^b, \mathbf{T}_2^c]. \end{aligned}$$

We would like to isolate the contributions to F_1 - and F_2 -term in the soft anomalous dimension. For this purpose it is convenient to regroup terms associated with $r(3)r(2)$ in the following way

$$\begin{aligned} r(3)r(2) &([\mathcal{C}(1, 2, 3) + \mathcal{C}(2, 1, 3)] g_{BB} + [\mathcal{C}(1, 3, 2) + \mathcal{C}(3, 1, 2)] g_{CC} \\ &\quad + [\mathcal{C}(1, 2, 3) - \mathcal{C}(2, 1, 3) + \mathcal{C}(1, 3, 2) - \mathcal{C}(3, 1, 2)] g_{+-} \\ &\quad + [\mathcal{C}(1, 2, 3) - \mathcal{C}(2, 1, 3) - \mathcal{C}(1, 3, 2) + \mathcal{C}(3, 1, 2)] g_{--}), \end{aligned} \quad (4.10)$$

where

$$\begin{aligned}
 g_{BB} &= g_B^+(3, 2, 1) + g_C^+(3, 1, 2) + g_B^-(3, 2, 1) + g_C^-(3, 1, 2), & g_{CC} &= g_{BB}|_{2 \leftrightarrow 3} \\
 g_{+-} &= g_B^+(3, 2, 1) - g_C^+(3, 1, 2), & g_{--} &= g_B^-(3, 2, 1) - g_C^-(3, 1, 2).
 \end{aligned} \tag{4.11}$$

Investigating the structure of color factors, we observe that only $\{g_A^-, g_{--}\}$ contribute to the F_1 -term in the soft anomalous dimension, whereas only $\{g_A^+, g_{BB}, g_{CC}\}$ contribute to the F_2 -term. The expressions for $\{g_A^-(1, 2, 3), g_{--}, g_A^+(1, 2, 3), g_{BB}\}$ are given in the following, which involve products of logarithms with classical polylogarithms up to weight four.

$$g_A^- = -\frac{8}{9} l_+ l_- h_3(1), \tag{4.12}$$

$$\begin{aligned}
 g_{--} &= -\frac{4}{9} \left[-6 l_- \mathcal{L}_4^c + 6 l_+ \mathcal{L}_4^d + 4 l_3 h_4^b(2) - 4 l_2 h_4^b(3) \right. \\
 &\quad - 3 l_- l_+ \mathcal{L}_3^b + 6 l_1 l_- \mathcal{L}_3^c - 6 l_1 l_+ \mathcal{L}_3^d \\
 &\quad + 3 l_1 l_- l_+ \mathcal{L}_2^b - l_- (3 l_1^2 + \pi^2) \mathcal{L}_2^c + l_+ (3 l_1^2 + \pi^2) \mathcal{L}_2^d \\
 &\quad \left. + l_2 l_3 l_- l_+ \mathcal{L}_1^a + \frac{1}{2} l_- l_+ (-3 l_1^2 + l_2^2 + l_3^2 + \pi^2) \mathcal{L}_1^b + l_1 l_- (l_1^2 + \pi^2) \mathcal{L}_1^c - l_1 l_+ (l_1^2 + \pi^2) \mathcal{L}_1^d \right],
 \end{aligned} \tag{4.13}$$

$$\begin{aligned}
 g_A^+ &= \frac{4}{9} l_1 \left[-6 \mathcal{L}_4^a - 6 l_+ \mathcal{L}_3^c - 6 l_- \mathcal{L}_3^d - 8 h_4^a(1) \right. \\
 &\quad - (-3 l_1^2 + 3 l_2^2 + 3 l_3^2 + \pi^2) \mathcal{L}_2^a - 6 l_2 l_3 \mathcal{L}_2^b \\
 &\quad \left. - 2 l_1 (l_1^2 + \pi^2) \mathcal{L}_1^a - l_+ (-3 l_1^2 + l_+^2 + \pi^2) \mathcal{L}_1^c - l_- (-3 l_1^2 + l_-^2 + \pi^2) \mathcal{L}_1^d \right],
 \end{aligned} \tag{4.14}$$

$$\begin{aligned}
 g_{BB} &= -\frac{4}{9} l_3 \left[-6 (\mathcal{L}_4^c + \mathcal{L}_4^d) - 6 l_3 \mathcal{L}_3^b + 6 l_1 (\mathcal{L}_3^c + \mathcal{L}_3^d) + 8 h_4^a(2) \right. \\
 &\quad + 6 l_1 l_3 \mathcal{L}_2^b + (-3 l_1^2 + 3 l_+ l_- - \pi^2) (\mathcal{L}_2^c + \mathcal{L}_2^d) \\
 &\quad \left. + 2 l_2 (l_2^2 + \pi^2) \mathcal{L}_1^a - l_3 (3 l_1^2 - 3 l_2^2 + l_3^2 + \pi^2) \mathcal{L}_1^b + l_1 (l_1^2 - 3 l_+ l_- + \pi^2) (\mathcal{L}_1^c + \mathcal{L}_1^d) \right].
 \end{aligned} \tag{4.15}$$

Here we define logarithms

$$l_1 = \ln \alpha_1, \quad l_2 = \ln \alpha_2, \quad l_3 = \ln \alpha_3, \quad l_+ = \ln \alpha_2 \alpha_3, \quad l_- = \ln \frac{\alpha_2}{\alpha_3}, \tag{4.16}$$

and basis of polylogarithms

$$\begin{aligned}
 \mathcal{L}_n^a &= \frac{1}{2} \left[\text{Li}_n \left(-\frac{\alpha_1}{\alpha_2 \alpha_3} \right) + \text{Li}_n \left(-\frac{\alpha_1 \alpha_3}{\alpha_2} \right) + \text{Li}_n \left(-\frac{\alpha_1 \alpha_2}{\alpha_3} \right) + \text{Li}_n (-\alpha_1 \alpha_2 \alpha_3) \right] \pm \left(\alpha \leftrightarrow \frac{1}{\alpha} \right) \\
 \mathcal{L}_n^b &= \frac{1}{2} \left[\text{Li}_n \left(-\frac{\alpha_1}{\alpha_2 \alpha_3} \right) - \text{Li}_n \left(-\frac{\alpha_1 \alpha_3}{\alpha_2} \right) - \text{Li}_n \left(-\frac{\alpha_1 \alpha_2}{\alpha_3} \right) + \text{Li}_n (-\alpha_1 \alpha_2 \alpha_3) \right] \pm \left(\alpha \leftrightarrow \frac{1}{\alpha} \right) \\
 \mathcal{L}_n^c &= \frac{1}{2} \left[\text{Li}_n \left(-\frac{\alpha_1}{\alpha_2 \alpha_3} \right) - \text{Li}_n (-\alpha_1 \alpha_2 \alpha_3) \right] \pm \left(\alpha \leftrightarrow \frac{1}{\alpha} \right) \\
 \mathcal{L}_n^d &= \frac{1}{2} \left[\text{Li}_n \left(-\frac{\alpha_1 \alpha_3}{\alpha_2} \right) - \text{Li}_n \left(-\frac{\alpha_1 \alpha_2}{\alpha_3} \right) \right] \pm \left(\alpha \leftrightarrow \frac{1}{\alpha} \right),
 \end{aligned} \tag{4.17}$$

where \pm stands for $+$ if n is odd, and $-$ if n is even. By construction, these basis are (anti-)symmetric under the transformation which inverts all α 's.

In addition, there are terms which depend on a single cusp angle. We group them together and introduce the following set of functions

$$\begin{aligned} h_3(i) &= -24 li_3(i), \\ h_4^a(i) &= 6 li_4(i) - 4 l_i li_3(i) + (l_i^2 + \pi^2) li_2(i), \quad h_4^b(i) = 72 li_4(i) + h_4^a(i), \end{aligned} \quad (4.18)$$

where

$$li_n(i) \equiv \frac{1}{2^n} \left[\text{Li}_n(\alpha_i^2) - \zeta_n - \frac{2}{n-1} \ln \alpha_i (\text{Li}_{n-1}(\alpha_i^2) - \zeta_{n-1}) \right] \pm \left(\alpha_i \leftrightarrow \frac{1}{\alpha_i} \right). \quad (4.19)$$

Again, \pm stands for $+$ if n is odd, and $-$ if n is even, $\forall n \in \{2, 3, 4\}$. In the special case where $n = 2$, the ζ_{n-1} term in (4.19) should be set to 0.

Let us emphasize that the basis of polylogarithms given in (4.16), (4.17) and (4.19) satisfy the following properties. Firstly, they are single-valued in the so-called *Euclidean region*, where $\alpha_1, \alpha_2, \alpha_3 > 0$. In particular the branch cuts on the positive real axis of α_i cancel in (4.19). Secondly, each member in the set of function we introduced, i.e.

$$\{l_1, l_2, l_3, \mathcal{L}_n^a, \mathcal{L}_n^b, \mathcal{L}_n^c \pm \mathcal{L}_n^d, li_n\}$$

is either symmetric or anti-symmetric under the transformation which inverts any set of cusp angle variables ($\alpha_i \rightarrow \alpha_i^{-1}, \forall i$). Moreover, the functions

$$\{l_+, l_-, \mathcal{L}_n^a, \mathcal{L}_n^b, \mathcal{L}_n^c, \mathcal{L}_n^d\}$$

are (anti-)symmetric under the exchange ($2 \leftrightarrow 3$). Given these nice properties, the form of the final result is highly constrained.

5 Discussion and outlook

In this paper we proposed and tested a new regularization scheme for computing the soft anomalous dimension matrix. We considered the ratio between the correlation function for n and $n - 1$ Wilson-line operators, which is free from IR divergences, provided that the n -th Wilson-line is dressed with an offshellness regulator. Based on this observation, we defined a renormalized quantity $\mathcal{S}_{0,\dots,1}^{\text{fin.}}$ that satisfies the renormalization group equation

$$\left[\mu \frac{\partial}{\partial \mu} + \beta(\alpha) \frac{\partial}{\partial \alpha} \right] \mathcal{S}_{0,\dots,1}^{\text{fin.}} = \Gamma_{\mathbf{n}-1} \mathcal{S}_{0,\dots,1}^{\text{fin.}} - \mathcal{S}_{0,\dots,1}^{\text{fin.}} \Gamma_{\mathbf{n}}. \quad (5.1)$$

This allows us to determine the soft anomalous dimension matrix for an arbitrary number of massive particles, by sequentially computing $\mathcal{S}_{0,1}, \mathcal{S}_{0,0,1}, \dots, \mathcal{S}_{0,\dots,1}$ and extracting their UV poles.

We motivated the regularization scheme by physical arguments, rather than providing a mathematical proof. We tested the novel method by demonstrating how the known one- and two-loop results are obtained within this setup. Employing the differential equations method, we note that calculations are simpler compared to the traditional setup where all Wilson lines are regulated in the IR. As a proof of principle, we evaluated one of the three-loop web diagrams that contributes to the three-Wilson-line soft anomalous dimension

matrix Γ_3 . Previously, this was out of reach of conventional methods. This contribution to the soft anomalous dimension matrix is computed here for the first time. A natural next step, beyond the scope of this paper, is to evaluate the other relevant Feynman diagrams contributing to this observable.

Our two-loop and sample three-loop calculations shed light on the new features that might appear in Γ_3 . The final formula for the two-loop soft anomalous dimension matrix depends on the following alphabet only,

$$\{1 - x_{12}, x_{12}, 1 + x_{12}, 1 - x_{13}, x_{13}, 1 + x_{13}, 1 - x_{23}, x_{23}, 1 + x_{23}\}. \quad (5.2)$$

Although this depends on three variables, the dependence is factorized, which implies that any function within this alphabet is a sum of products of single-variable functions. In-contrast, the web diagrams we computed involve the thirteen-letter alphabet (3.24). Compared to (5.2), this involves the following new alphabet letters,

$$\{x_{12} + x_{13}x_{23}, x_{13} + x_{12}x_{23}, x_{23} + x_{12}x_{13}, 1 + x_{12}x_{13}x_{23}\}. \quad (5.3)$$

This implies more complicated and richer structures for the transcendental functions.¹ (At the same time, it is interesting that \mathcal{F}_{122} is given by products of logarithms with classical polylogarithms whose arguments are drawn from a small set of variables.) These observations motivate a more systematic study on the function space of multi-line soft anomalous dimension, which will be valuable input for bootstrap approaches.

A further interesting direction is to investigate the web function in $\mathcal{N} = 4$ super Yang-Mills (sYM). At the three-loop order, the difference between the corresponding soft anomalous dimension matrices is captured by simpler, matter-dependent terms. Interestingly, those terms have been observed to exhibit an universal iterative structure [11] in the two-line case, namely

$$\Gamma_{\text{cusp}}(\phi) = C_R \frac{a}{\pi} \left[\Omega(\phi) + \frac{a}{\pi} C_A \Omega_A(\phi) + \left(\frac{a}{\pi}\right)^2 C_A^2 \Omega_{AA}(\phi) \right] + \mathcal{O}(a_s^4). \quad (5.4)$$

The angle-dependent function Ω 's are independent of the particle content of the gauge theory, whereas n_f - and n_s -dependence can be associated with an effective coupling constant a . (This holds up to three loops; at four loops terms proportional to the quartic Casimir color component break this pattern [12].) It would be interesting to see whether such a pattern exists for the tripole function $F_1^{(2)}$ and $F_1^{(3)}$ as well. Finally, in addition to considering the standard Wilson line operator, it is possible to consider the (locally supersymmetric) Maldacena operator, which includes a term coupling to scalars. This leads to additional sets of angle parameters in the flavour space of scalars that the correlation functions depend on, and that can be used to organize calculations and define novel limits [54].

Acknowledgments

We would like to thank Einan Gardi and Zelong Liu for enlightening discussions. This research received funding from the European Research Council (ERC) under the European

¹Also, the result of ref. [53] for the soft anomalous dimension matrix for one massive and two massless particles may suggest the appearance of further alphabet letters.

Union’s Horizon 2020 research and innovation programme (grant agreement No 725110), *Novel structures in scattering amplitudes*. KY is supported by the National Natural Science Foundation of China under Grant No. 12357077 and would like to thank the sponsorship from Yangyang Development Fund. CM has been partially supported by the Italian Ministry of University and Research (MUR) through grant PRIN20172LNEEZ and by Compagnia di San Paolo through grant TORPS1921EX-POST2101.

A Asymptotic expansion by regions for $\mathcal{S}_{\delta,\delta,1}$ at two-loop level

We perform the asymptotic expansion in δ for the two-loop soft function $\mathcal{S}_{\delta,\delta,1}$. Our analysis is based on the method of regions approach [55], and provides a proof-of-concept example for the factorization property as stated in eq. (2.18).

The two-loop soft function receives contributions from two types of diagrams as illustrated in figure 2. The dark black line represents the ‘hard offshell’ Wilson line for which the IR cutoff parameter is set to 1. In the limit where $\delta \rightarrow 0$, the asymptotic expansion for a given diagram has the schematic form:

$$I(\delta, \delta, 1; \epsilon) = \sum_n \delta^{-n\epsilon} [a_{n,0}(\epsilon) + a_{n,1}(\epsilon) \delta + \dots] \quad (\text{A.1})$$

where we have omitted the kinematic dependence on $v_i \cdot v_j$. Only the leading terms with coefficients $a_{n,0}(\epsilon)$ could be responsible for the singularity in the δ -parameter. We perform the expansion by regions using MATHEMATICA package `asy2.m` [56, 57] and thus predicting the leading behaviour for each two-loop diagrams.

First we consider figure 2 (b) with triple gluon interaction

$$I_{2b} = \int \frac{d^d k_1}{i\pi^{d/2}} \frac{d^d k_2}{i\pi^{d/2}} \frac{\sum_{k=7}^9 n_k D_k}{D_1 D_2 D_3 D_4 D_5 D_6} \quad \text{where}$$

$$D_1 = v_1 \cdot k_1 + \delta, \quad D_2 = v_2 \cdot k_2 + \delta, \quad D_3 = -v_3 \cdot (k_1 + k_2) + 1,$$

$$D_4 = k_1^2, \quad D_5 = k_2^2, \quad D_6 = (k_1 + k_2)^2, \quad D_7 = k_1 \cdot v_3,$$

$$D_8 = k_1 \cdot v_2, \quad D_9 = k_2 \cdot v_1. \quad (\text{A.2})$$

Using `asy2.m` to expand in small parameter δ , we identify all potential singular regions, characterized by region vectors

$$\begin{aligned} u_1 &= \{0, 1, 0, 0, 2, 0, 0, 0, 1\}, & u_2 &= \{0, 0, 0, 0, 0, 0, 0, 0, 0\}, \\ u_3 &= \{1, 1, 0, 2, 2, 2, 1, 1, 1\}, & u_4 &= \{1, 0, 0, 2, 0, 0, 1, 1, 0\}, \end{aligned} \quad (\text{A.3})$$

where each vector u_I specifies the scales of propagators $\{D_1, \dots, D_9\} \sim \delta^{u_I}$ in a given region. Further investigating the corresponding loop momentum scaling behaviours, we find

$$\begin{aligned} u_1 : k_2 - \text{soft}. & & k_2^\mu \sim \delta, k_1^\mu \sim 1 & & u_2 : \text{hard}. & & (k_1^\mu, k_2^\mu) \sim 1 \\ u_3 : (k_1, k_2) - \text{soft}. & & (k_1^\mu, k_2^\mu) \sim \delta & & u_4 : k_1 - \text{soft}. & & k_1^\mu \sim \delta, k_2^\mu \sim 1 \end{aligned} \quad (\text{A.4})$$

The scales of integral I_{2b} in the four regions are given by

$$\delta^{1-2\epsilon}, \quad \delta^0, \quad \delta^{1-4\epsilon}, \quad \delta^{1-2\epsilon}, \quad (\text{A.5})$$

respectively. Hence u_2 is the only *leading* region in the asymptotic limit and contributes to the $a_{0,0}$ term in the expansion. This is a hard region where all the loop momenta are order 1 and the δ -regulators should be set to zero. Thus we conclude, for the triple-gluon diagram,

$$I_{2b}(\delta, \delta, 1; \epsilon) = I_{2b}(0, 0, 1; \epsilon) + O(\delta) \tag{A.6}$$

Next we proceed with the ladder-type diagrams in figure 3. Following the same procedure, we can show that the hard region is the only *leading* region for diagrams in figure 3 (a),(c),(d),(f), whose asymptotic expansion behaviours are the same as (A.6).

The remaining two diagrams, figure 3(b) and 3(e), are related by switching v_1 with v_2 . Figure 3(b) defines an integral $I_{3b} \equiv F_{1,1,1,1,1,1,0,0,0}$ which belongs to the following integral family

$$F_{a_1, \dots, a_9} \equiv \int \frac{d^d k_1}{i\pi^{d/2}} \frac{d^d k_2}{i\pi^{d/2}} \frac{1}{\prod_{i=1}^9 D_i^{a_i}} \quad \text{where}$$

$$D_1 = v_1 \cdot k_1 + \delta, \quad D_2 = v_2 \cdot (k_1 + k_2) + \delta, \quad D_3 = v_2 \cdot k_1 + \delta, \quad D_4 = -v_3 \cdot k_2 + 1,$$

$$D_5 = k_1^2, \quad D_6 = k_2^2, \quad D_7 = (k_1 + k_2)^2, \quad D_8 = k_1 \cdot v_3, \quad D_9 = k_2 \cdot v_1 \tag{A.7}$$

Allowing arbitrary propagator indices, the potential singular regions for the family of integrals are specified by the following vectors

$$u_1 = \{0, 1, 0, 0, 0, 0, 2, 0, 0\}, \quad u_2 = \{0, 0, 0, 0, 0, 0, 0, 0, 0\},$$

$$u_3 = \{1, 1, 1, 0, 2, 2, 2, 1, 1\}, \quad u_4 = \{1, 0, 1, 0, 2, 0, 0, 1, 0\}. \tag{A.8}$$

For the specific integral $I_{3b} = F_{1,1,1,1,1,1,0,0,0}$, u_1, u_3 are subleading by power counting, which we do not discuss. u_2 is the **hard** region. u_4 is the k_1 -**soft** region, where $k_1^\mu \sim \delta$, $k_2^\mu \sim 1$, and I_{3b} reduces to the product of two one-loop integrals

$$I_{3b} \stackrel{u_4}{\cong} \left[\int \frac{d^d k_1}{i\pi^{d/2}} \frac{1}{D_1 D_3 D_5} \right] \times \left[\int \frac{d^d k_2}{i\pi^{d/2}} \frac{1}{[v_2 \cdot k_2] [-v_3 \cdot k_2 + 1] [k_2^2]} \right]$$

$$\equiv I_{v_{1,2}}(\delta, \delta; \epsilon) \times I_{v_{2,3}}(0, 1; \epsilon) \tag{A.9}$$

where $I_{v_{1,2}}(\delta, \delta) = \delta^{-2\epsilon} I_{v_{1,2}}(1, 1)$ is a single-scale integral. Hence the ladder integral I_{3b} has the following asymptotic expansion:

$$I_{3b}(\delta, \delta, 1; \epsilon) = \delta^{-2\epsilon} I_{v_{1,2}}(1, 1; \epsilon) I_{v_{2,3}}(0, 1; \epsilon) + I_{3b}(0, 0, 1; \epsilon) + O(\delta) \tag{A.10}$$

where only the first term contains logarithmic singularity in the δ -parameter.

In summary, we have investigated the behaviours of all three-line diagrams that contribute to $\mathcal{S}_{\delta, \delta, 1}$ at two-loop level, in the limit where $\delta \rightarrow 0$. The only diagrams that are singular in this limit are figure 3(b) and 3(e), where such singularity factorizes in terms of one-loop two-line integrals. The structure of the asymptotic expansions in (A.6), (A.9) verifies the following statement

$$\mathcal{S}_{\delta, \delta, 1}^{(2)} = \mathcal{S}_{\delta, \delta}^{(1)} \mathcal{S}_{0,0,1}^{(1)} + \mathcal{S}_{0,0,1}^{(2)} + \mathcal{O}(\delta) \tag{A.11}$$

which holds for the three-line diagrams at two-loop level, where $\mathcal{S}^{(k)}$ denotes the fixed-order expansion for the soft function at k -loop order. Hereby we have tested the validity of eq. (2.18) through method-of-regions analysis on concrete examples. In section 3 we will further test our new method by explicit calculation of the two-loop soft anomalous dimension.

Open Access. This article is distributed under the terms of the Creative Commons Attribution License ([CC-BY4.0](https://creativecommons.org/licenses/by/4.0/)), which permits any use, distribution and reproduction in any medium, provided the original author(s) and source are credited.

References

- [1] I.A. Korchemskaya and G.P. Korchemsky, *High-energy scattering in QCD and cross singularities of Wilson loops*, *Nucl. Phys. B* **437** (1995) 127 [[hep-ph/9409446](#)] [[INSPIRE](#)].
- [2] N. Kidonakis and G.F. Sterman, *Subleading logarithms in QCD hard scattering*, *Phys. Lett. B* **387** (1996) 867 [[INSPIRE](#)].
- [3] N. Kidonakis and G.F. Sterman, *Resummation for QCD hard scattering*, *Nucl. Phys. B* **505** (1997) 321 [[hep-ph/9705234](#)] [[INSPIRE](#)].
- [4] L.J. Dixon, L. Magnea and G.F. Sterman, *Universal structure of subleading infrared poles in gauge theory amplitudes*, *JHEP* **08** (2008) 022 [[arXiv:0805.3515](#)] [[INSPIRE](#)].
- [5] T. Becher and M. Neubert, *Infrared singularities of scattering amplitudes in perturbative QCD*, *Phys. Rev. Lett.* **102** (2009) 162001 [*Erratum ibid.* **111** (2013) 199905] [[arXiv:0901.0722](#)] [[INSPIRE](#)].
- [6] E. Gardi and L. Magnea, *Factorization constraints for soft anomalous dimensions in QCD scattering amplitudes*, *JHEP* **03** (2009) 079 [[arXiv:0901.1091](#)] [[INSPIRE](#)].
- [7] O. Almeliid, C. Duhr and E. Gardi, *Three-loop corrections to the soft anomalous dimension in multileg scattering*, *Phys. Rev. Lett.* **117** (2016) 172002 [[arXiv:1507.00047](#)] [[INSPIRE](#)].
- [8] J.M. Henn and B. Mistlberger, *Four-gluon scattering at three loops, infrared structure, and the Regge limit*, *Phys. Rev. Lett.* **117** (2016) 171601 [[arXiv:1608.00850](#)] [[INSPIRE](#)].
- [9] F. Caola et al., *Three-loop helicity amplitudes for four-quark scattering in massless QCD*, *JHEP* **10** (2021) 206 [[arXiv:2108.00055](#)] [[INSPIRE](#)].
- [10] A. Grozin, J.M. Henn, G.P. Korchemsky and P. Marquard, *Three loop cusp anomalous dimension in QCD*, *Phys. Rev. Lett.* **114** (2015) 062006 [[arXiv:1409.0023](#)] [[INSPIRE](#)].
- [11] A. Grozin, J.M. Henn, G.P. Korchemsky and P. Marquard, *The three-loop cusp anomalous dimension in QCD and its supersymmetric extensions*, *JHEP* **01** (2016) 140 [[arXiv:1510.07803](#)] [[INSPIRE](#)].
- [12] R. Brüser, C. Dlapa, J.M. Henn and K. Yan, *Full angle dependence of the four-loop cusp anomalous dimension in QED*, *Phys. Rev. Lett.* **126** (2021) 021601 [[arXiv:2007.04851](#)] [[INSPIRE](#)].
- [13] A. Mitov, G.F. Sterman and I. Sung, *The massive soft anomalous dimension matrix at two loops*, *Phys. Rev. D* **79** (2009) 094015 [[arXiv:0903.3241](#)] [[INSPIRE](#)].
- [14] A. Ferroglia, M. Neubert, B.D. Pecjak and L.L. Yang, *Two-loop divergences of scattering amplitudes with massive partons*, *Phys. Rev. Lett.* **103** (2009) 201601 [[arXiv:0907.4791](#)] [[INSPIRE](#)].
- [15] A. Mitov, G.F. Sterman and I. Sung, *Computation of the soft anomalous dimension matrix in coordinate space*, *Phys. Rev. D* **82** (2010) 034020 [[arXiv:1005.4646](#)] [[INSPIRE](#)].
- [16] Y.-T. Chien, M.D. Schwartz, D. Simmons-Duffin and I.W. Stewart, *Jet physics from static charges in AdS*, *Phys. Rev. D* **85** (2012) 045010 [[arXiv:1109.6010](#)] [[INSPIRE](#)].

- [17] S. Catani and M.H. Seymour, *A general algorithm for calculating jet cross-sections in NLO QCD*, *Nucl. Phys. B* **485** (1997) 291 [[hep-ph/9605323](#)] [[INSPIRE](#)].
- [18] A. Bassetto, M. Ciafaloni and G. Marchesini, *Jet structure and infrared sensitive quantities in perturbative QCD*, *Phys. Rept.* **100** (1983) 201 [[INSPIRE](#)].
- [19] A.V. Kotikov, *Differential equations method: new technique for massive Feynman diagrams calculation*, *Phys. Lett. B* **254** (1991) 158 [[INSPIRE](#)].
- [20] Z. Bern, L.J. Dixon and D.A. Kosower, *Dimensionally regulated pentagon integrals*, *Nucl. Phys. B* **412** (1994) 751 [[hep-ph/9306240](#)] [[INSPIRE](#)].
- [21] T. Gehrmann and E. Remiddi, *Differential equations for two loop four point functions*, *Nucl. Phys. B* **580** (2000) 485 [[hep-ph/9912329](#)] [[INSPIRE](#)].
- [22] J.M. Henn, *Multiloop integrals in dimensional regularization made simple*, *Phys. Rev. Lett.* **110** (2013) 251601 [[arXiv:1304.1806](#)] [[INSPIRE](#)].
- [23] J. Henn and D. Simmons-Duffin, *Differential equations for two-loop web functions*, unpublished, (2011).
- [24] C.W. Milloy, *Infrared divergences in scattering amplitudes from correlators of Wilson lines*, Ph.D. thesis, Edinburgh U., Edinburgh, U.K. (2020) [[INSPIRE](#)].
- [25] J.G.M. Gatheral, *Exponentiation of eikonal cross-sections in non-Abelian gauge theories*, *Phys. Lett. B* **133** (1983) 90 [[INSPIRE](#)].
- [26] J. Frenkel and J.C. Taylor, *Non-Abelian eikonal exponentiation*, *Nucl. Phys. B* **246** (1984) 231 [[INSPIRE](#)].
- [27] G.F. Sterman, *Infrared divergences in perturbative QCD*, *AIP Conf. Proc.* **74** (1981) 22 [[INSPIRE](#)].
- [28] J.C. Collins and G.F. Sterman, *Soft partons in QCD*, *Nucl. Phys. B* **185** (1981) 172 [[INSPIRE](#)].
- [29] A. Sen, *Asymptotic behavior of the wide angle on-shell quark scattering amplitudes in non-Abelian gauge theories*, *Phys. Rev. D* **28** (1983) 860 [[INSPIRE](#)].
- [30] S.V. Ivanov, G.P. Korchemsky and A.V. Radyushkin, *Infrared asymptotics of perturbative QCD: contour gauges*, *Yad. Fiz.* **44** (1986) 230 [[INSPIRE](#)].
- [31] J.C. Collins, D.E. Soper and G.F. Sterman, *Soft gluons and factorization*, *Nucl. Phys. B* **308** (1988) 833 [[INSPIRE](#)].
- [32] L. Magnea and G.F. Sterman, *Analytic continuation of the Sudakov form-factor in QCD*, *Phys. Rev. D* **42** (1990) 4222 [[INSPIRE](#)].
- [33] G.P. Korchemsky and A.V. Radyushkin, *Infrared factorization, Wilson lines and the heavy quark limit*, *Phys. Lett. B* **279** (1992) 359 [[hep-ph/9203222](#)] [[INSPIRE](#)].
- [34] G.F. Sterman and M.E. Tejeda-Yeomans, *Multiloop amplitudes and resummation*, *Phys. Lett. B* **552** (2003) 48 [[hep-ph/0210130](#)] [[INSPIRE](#)].
- [35] S.M. Aybat, L.J. Dixon and G.F. Sterman, *The two-loop soft anomalous dimension matrix and resummation at next-to-next-to leading pole*, *Phys. Rev. D* **74** (2006) 074004 [[hep-ph/0607309](#)] [[INSPIRE](#)].
- [36] A.V. Manohar and M.B. Wise, *Heavy quark physics*, Cambridge University Press, Cambridge, U.K. (2000) [[DOI:10.1017/cbo9780511529351](#)].
- [37] S. Catani, *The singular behavior of QCD amplitudes at two loop order*, *Phys. Lett. B* **427** (1998) 161 [[hep-ph/9802439](#)] [[INSPIRE](#)].

- [38] T. Becher and M. Neubert, *On the structure of infrared singularities of gauge-theory amplitudes*, *JHEP* **06** (2009) 081 [*Erratum ibid.* **11** (2013) 024] [[arXiv:0903.1126](#)] [[INSPIRE](#)].
- [39] E. Gardi and L. Magnea, *Infrared singularities in QCD amplitudes*, *Nuovo Cim. C* **32N5-6** (2009) 137 [[arXiv:0908.3273](#)] [[INSPIRE](#)].
- [40] S. Catani and M.H. Seymour, *The dipole formalism for the calculation of QCD jet cross-sections at next-to-leading order*, *Phys. Lett. B* **378** (1996) 287 [[hep-ph/9602277](#)] [[INSPIRE](#)].
- [41] E. Gardi and C.D. White, *General properties of multiparton webs: proofs from combinatorics*, *JHEP* **03** (2011) 079 [[arXiv:1102.0756](#)] [[INSPIRE](#)].
- [42] E. Gardi, J.M. Smillie and C.D. White, *On the renormalization of multiparton webs*, *JHEP* **09** (2011) 114 [[arXiv:1108.1357](#)] [[INSPIRE](#)].
- [43] E. Gardi, J.M. Smillie and C.D. White, *The non-Abelian exponentiation theorem for multiple Wilson lines*, *JHEP* **06** (2013) 088 [[arXiv:1304.7040](#)] [[INSPIRE](#)].
- [44] G. Falcioni et al., *Multiple gluon exchange webs*, *JHEP* **10** (2014) 010 [[arXiv:1407.3477](#)] [[INSPIRE](#)].
- [45] G.P. Korchemsky and A.V. Radyushkin, *Renormalization of the Wilson loops beyond the leading order*, *Nucl. Phys. B* **283** (1987) 342 [[INSPIRE](#)].
- [46] A.J.N. Waelkens, *Calculation of webs in non-Abelian gauge theories using unitarity cuts*, Ph.D. thesis, Edinburgh U., Edinburgh, U.K. (2017) [[INSPIRE](#)].
- [47] J. Klappert, F. Lange, P. Maierhöfer and J. Usovitsch, *Integral reduction with Kira 2.0 and finite field methods*, *Comput. Phys. Commun.* **266** (2021) 108024 [[arXiv:2008.06494](#)] [[INSPIRE](#)].
- [48] C. Meyer, *Algorithmic transformation of multi-loop master integrals to a canonical basis with CANONICA*, *Comput. Phys. Commun.* **222** (2018) 295 [[arXiv:1705.06252](#)] [[INSPIRE](#)].
- [49] J. Henn, B. Mistlberger, V.A. Smirnov and P. Wasser, *Constructing d -log integrands and computing master integrals for three-loop four-particle scattering*, *JHEP* **04** (2020) 167 [[arXiv:2002.09492](#)] [[INSPIRE](#)].
- [50] C. Dlapa, J. Henn and K. Yan, *Deriving canonical differential equations for Feynman integrals from a single uniform weight integral*, *JHEP* **05** (2020) 025 [[arXiv:2002.02340](#)] [[INSPIRE](#)].
- [51] L.J. Dixon, E. Gardi and L. Magnea, *On soft singularities at three loops and beyond*, *JHEP* **02** (2010) 081 [[arXiv:0910.3653](#)] [[INSPIRE](#)].
- [52] R.N. Lee, *Libra: a package for transformation of differential systems for multiloop integrals*, *Comput. Phys. Commun.* **267** (2021) 108058 [[arXiv:2012.00279](#)] [[INSPIRE](#)].
- [53] Z.L. Liu and N. Schalch, *Infrared singularities of multileg QCD amplitudes with a massive parton at three loops*, *Phys. Rev. Lett.* **129** (2022) 232001 [[arXiv:2207.02864](#)] [[INSPIRE](#)].
- [54] D. Correa, J. Henn, J. Maldacena and A. Sever, *The cusp anomalous dimension at three loops and beyond*, *JHEP* **05** (2012) 098 [[arXiv:1203.1019](#)] [[INSPIRE](#)].
- [55] M. Beneke and V.A. Smirnov, *Asymptotic expansion of Feynman integrals near threshold*, *Nucl. Phys. B* **522** (1998) 321 [[hep-ph/9711391](#)] [[INSPIRE](#)].
- [56] A. Pak and A. Smirnov, *Geometric approach to asymptotic expansion of Feynman integrals*, *Eur. Phys. J. C* **71** (2011) 1626 [[arXiv:1011.4863](#)] [[INSPIRE](#)].
- [57] B. Jantzen, A.V. Smirnov and V.A. Smirnov, *Expansion by regions: revealing potential and Glauber regions automatically*, *Eur. Phys. J. C* **72** (2012) 2139 [[arXiv:1206.0546](#)] [[INSPIRE](#)].